EASR

Engineering and Applied Science Research

https://www.tci-thaijo.org/index.php/easr/index

Published by the Faculty of Engineering, Khon Kaen University, Thailand

Ensemble of four metaheuristic using a weighted sum technique for aircraft wing design

Kittinan Wansasueb*[1)], Sujin Bureerat[1)] and Sumit Kumar[2)]

[1)]Sustainable Infrastructure Research and Development Centre, Department of Mechanical Engineering, Faculty of Engineering, Khon Kaen University, Khon Kaen 40002, Thailand
[2)]Department of Mechanical Engineering, GPERI, Gujarat Technological University, Gujarat, India

Received 6 October 2020
Revised 31 October 2020
Accepted 11 November 2020

Abstract

Recently, metaheuristics (MHs) have become increasingly popular in real-world engineering applications such as in the design of airframes structures and aeroelastic designs owing to its simple, flexible, and efficient nature. In this study, a novel hybrid algorithm is termed as Ensemble of Genetic algorithm, Grey wolf optimizer, Water cycle algorithm and Population base increment learning using Weighted sum (E-GGWP-W), based on the successive archive methodology of the weighted population has been proposed to solve the aircraft composite wing design problem. Four distinguished algorithms viz. a Genetic algorithm (GA), a Grey wolf optimizer (GWO), a Water cycle algorithm (WCA), and Population base increment learning (PBIL) were used as ingredients of the proposed algorithm. The considered wing design problem is posed for overall weight minimization subject to several aeroelastic and structural constraints along with multiple discrete design variables to ascertain its viability for real-world applications. The algorithms are validated through the standard test functions of the CEC-RW-2020 test suite and composite Goland wing aeroelastic optimization. To check the performance, the proposed algorithm is contrasted with eight well established and newly developed MHs. Finally, a statistical analysis is done by performing Friedman's rank test and allocating respective ranks to the algorithms. Based on the outcome, it has been observed that the suggested algorithm outperforms the others.

Keywords: Optimisation algorithm, Aeroelastic design, Composite wing, Flutter speed, Metaheuristics

1. Introduction

Nowadays, the aircraft industries and researchers are continuously investigating highly fuel-efficient and lightweight wing designs to meet the global challenges of travel demand, carbon footprint reduction, and sustainability. Additionally, as per the new regulation, the aeroelastic characteristics of any new aircraft design proposed by industries should be detailed and must get its airworthiness approval from the global aviation organizations, such as Federal Aviation Administration (FAA), European Aviation Safety Agency (EASA), etc., before its field test and commercialization [1]. It is therefore imperative to incorporate the simulation techniques for aeroelastic traits calculation in the aircraft design process itself, to reduce the consumption of experimental resources (case; time, cost, etc.) and to ensure that the final airframe design can meet the standards. Under the purview of the aircraft system, the mutual interaction between aerodynamic forces and elastic structure during the operation of aircraft is termed as Aeroelasticity, which is typically present in terms of critical velocity or effectiveness. However, aircraft performance cannot be assured by only meeting the avionic standards, and thus there is a requirement of optimal design which is economical, efficient, and simultaneously fulfills the environmental regulations. Numerous aircraft wing optimization studies (both single and multi-objective) have been conducted so far by scholars with typical objectives like structural weight minimization, high strength/stiffness, low cost, and some other aeroelastic characteristics like flutter stability, gust response, maneuver loads, lift, drag, etc.[2]. The design variable often considered in these studies is the location of wing part, thickness, or topology, etc., while, in composites structures optimization problem, fiber/matrix material, layers number, stacking sequence, ply orientation, layer thickness, and fiber volume fraction are often accounted for [2-5]. With this design procedure, the optimal wing solution can be found and lead to a further decision-making process in case of multi-objective problems.

Real-world design problems are often complex, large, challenging, and have a diverse framework that makes conventional methods like calculus-based techniques and enumerative techniques either fails to solve these complex problems or consume too much time [6]. Contrarily, metaheuristics (MHs) are powerful and robust gradient-free stochastic optimization methods employed for various numerical and combinatorial optimization problem solutions [7]. Typically, metaheuristics are adapted for sophisticated problems like discrete, discontinuous, noisy, dynamic, and non-differentiable which cause computation cost and time required extravagant and also occasionally impossible to get a solution. In recent years due to its remarkable effective mechanisms and tools, ease, versatility, derivation-free framework, and local optimum escape characteristics, MHs have moved into the limelight which made it the most popular technique for solving various real-world intricate problems [8]. For example, in mechanical design issues [9-17], in reliability-based design [1, 18] and for manufacturing operations [19, 20] numerous MHs were investigated such as particle swarm optimization (PSO), artificial bee colony (ABC), ant lion optimizer (ALO), multi-verse optimizer (MVO), salp swarm algorithm (SSA), grasshopper

*Corresponding author.
Email address: kittinan_w@kkumail.com
doi: 10.14456/easr.2021.41

optimization algorithm (GOA), dragonfly optimizer (DO), moth-flame optimization algorithm (MFO), grey wolf optimizer (GWO), water cycle algorithm (WCA), butterfly optimization algorithm (BOA), spotted hyena optimization algorithm (SHOA), modified adaptive differential evolution (MADE), Harris's Hawk optimizer (HHO), the hybrid algorithm including the hybrid between Nelder-Mead local search algorithm (NM) and whale optimization algorithm (WOA) into a novel hybrid whale-Nelder-Mead algorithm (HWOANM). Apart from MHs applications in the design procedure, these study also performed their comparative analysis that demonstrates their efficacy in resolving complex engineering design problems.

In the last four decades, MHs have been widely investigated for aircraft design problems such as winglet design optimization using multi-Island genetic algorithm optimization (MOGA-II) [21], laminate Carbon fibre wing box design using genetic algorithm (GA) [22], Improved Particle Swarm Optimization (PSO) with robust aerodynamic design [23], or even seen applications in the aircraft engines modelling and controller design [24]. So, it would not be wrong to say that the use of MHs is prevalent in modern applications of computational intelligence and these are the preferred methodology for any engineering design optimization problem.

Nevertheless, as per the prominent 'No Free Lunch' hypothesis [25], it is impossible for an MH to solve every problem effectively and efficiently. In a specific design issue, an MH may yield a good result, but still, the same strategy might generate a feeble result in another challenge [26]. To put it another way, there is no MH which provides optimal response for every problem. Hertz and de Werra [27] for example, claimed that tabu search (TS) in graph colouring problem is far nicer than simulated annealing (SA). In contrast, SA is better than TS in a lot-sizing problem, as per Kuik et al. [28]. However, Lee and Kim [29] described that TS and SA were equally efficient in a project scheduling problem. Furthermore, Yang [30] argued that there is no accepted method for contrasting the performance of different MHs. Consequently, discovering new, more powerful MHs is an active subject [31, 32]. Notably, Mernik et al. [33] figured out a couple of misconceptions in MH comparison. Eventually, Crepinsek et al. [34] cautioned that a meaningful comparison between the different MHs is extremely difficult.

One of the biggest disadvantages of many of these MHs, such as GAs and SA, is their sluggish convergence rate, which leads to high computational costs. Another shortcoming is the likelihood of the solution to be stuck in a local optimum like in Particle Swarm Optimisation (PSO), Tabu search (TS), Hirschberg–Sinclair algorithm (HS), and Ant colony optimization (ACO). To overcome these limitations, the emergence of hybridized, modified, and improved MHs is thus rising drastically for incorporating their more beneficial attributes [35, 36]. Moreover, for MHs the dynamic balance between global diversification and local intensification is of great importance [7, 8]. In principle, the terminology diversification corresponds to search space exploration, while the expression intensification leads to the utilization of the cumulative search knowledge. As mentioned, the harmony between the diversification and intensification is crucial because the former helps in promptly identifying the high-quality solutions regions in the search arena whereas the latter leads in minimal time in search areas which are either already being explored or that do not offer high-quality solutions [7, 8, 35, 36]. A quite burning question today is the quest for even more potent methods. The emergence of novel hybridized MHs is thus rising drastically. Thousands of MHs were implemented over the last few centuries by various researchers for engineering design optimization problems; however, this field has not been properly addressed until now.

In search of an efficient algorithm and to overcome the above-mentioned limitations of MHs, in this article the authors proposed and investigated a novel hybrid MH named as Ensemble of Genetic algorithm, Grey wolf optimiser, Water cycle algorithm, and Population base increment learning using Weighted sum (E-GGWP-W) to solve the composite wing optimization design issue. The details of the proposed hybrid algorithm are discussed in the following sections. The composite wing structural weight is considered as an objective function which is subjected to numerous aeroelastic and structural constraints with discrete design variables. The details of the investigated aeroelastic problem are illustrated in the Aeroelastic design problem section of this paper. For performance evaluation, the proposed algorithm is explored for two problem sets, aeroelastic optimization and the benchmark constrained mechanical test functions in the CEC-RW-2020 test suit [37]. The statistical test is performed and the mean, standard deviation results were compared with other state-of-the-art optimizers from the literature followed by Friedman's rank test to rank each algorithm. Outcomes from the computational experiment are represented and discussed in the Results section followed by the conclusive remark and future scope in the last section.

2. Ensemble of four metaheuristics via the weighted sum technique

A typical constrained single-objective optimization problem can be written as:

$$\min_{\mathbf{x}} \mathrm{f}(\mathbf{x}) \tag{1}$$

Subject to $\mathrm{g_i} \leq 0$

$$\mathbf{x}_\mathrm{L} \leq \mathbf{x} \leq \mathbf{x}_\mathrm{U}$$

where $\mathbf{x}$ is a solution vector containing n design variables, f is an objective function to be minimized, g_i is the constrained function to be handle and $\mathbf{x}_L$ and $\mathbf{x}_U$ are the lower and upper bounds of $\mathbf{x}$, respectively.

2.1 Genetic algorithm

Genetic algorithm (GA) is the most popular MH in solving the real-world design problems among all existing algorithms available in the literature. It was initially introduced in 1975 by John H. Holland [38, 39] and from that, this algorithm has been explored for every known discipline of engineering and science till now. Fundamentally GA is the population-based evolutionary algorithm that initializes the random solutions stochastically in the design space and then guides them towards the optimum. The algorithm performs its computation based on the principles of natural selection and genetics which is inspired by biological evolution [40]. The population is first randomly selected, then crossover is performed that enables the formation of superior offspring with a combination of best genes from individuals. Also, some of the child populations go through a mutation that adds diversity in the population and increasing the exploration potential of the search algorithm, while the probability of crossover and mutation were set as 0.88 and 0.05 [41], respectively.

2.2 Grey-wolf optimizer

Grey-wolf optimizer (GWO) is a recently introduced algorithm by S. Mirjalili et al. [26] which imitates the social hierarchy and hunting behaviour of a group of grey wolves. This method requires three controlling parameters viz. fittest solution called alpha (α), the second and third-best solutions termed as beta (β), and delta (δ) respectively, that control the direction of the search and solutions updating process. Rest candidate solutions are called omega (ω) which follow the other three wolves of the hierarchy. GWO works on three hunting processes of pray by wolves group i.e. searching, encircling, and attacking. The mathematical model of GWO can be represented as follows:

$$\mathrm{D}_{\alpha} = |\mathrm{C}_{\alpha} \times \mathbf{x}_{\alpha} - \mathbf{x}| \tag{2}$$

$$\mathrm{D}_{\beta} = |\mathrm{C}_{\beta} \times \mathbf{x}_{\beta} - \mathbf{x}| \tag{3}$$

$$\mathrm{D}_{\delta} = |\mathrm{C}_{\delta} \times \mathbf{x}_{\delta} - \mathbf{x}| \tag{4}$$

$$\mathbf{x}_1 = \mathbf{x}_{\alpha} - \mathrm{A}_{\alpha} \times \mathrm{D}_{\alpha} \tag{5}$$

$$\mathbf{x}_2 = \mathbf{x}_{\beta} - \mathrm{A}_{\beta} \times \mathrm{D}_{\beta} \tag{6}$$

$$\mathbf{x}_3 = \mathbf{x}_{\delta} - \mathrm{A}_{\delta} \times \mathrm{D}_{\delta} \tag{7}$$

$$\mathbf{x}_{\mathrm{GWO}}^{\mathrm{iter}+1} = (\mathbf{x}_1 + \mathbf{x}_2 + \mathbf{x}_3)/3 \tag{8}$$

Where $\mathrm{A}_{\alpha,\beta,\delta} = 2 \times \mathrm{a} \times \mathrm{rand}_{\alpha,\beta,\delta} - \mathrm{a}$
$\mathrm{C}_{\alpha,\beta,\delta} = 2 \times \mathrm{rand}_{\alpha,\beta,\delta}$
$\mathrm{a} = 2 - \mathrm{iteration} \times (\frac{2}{\mathrm{total\ iteration}})$

2.3 Water cycle algorithm

The water cycle algorithm (WCA) was introduced in 2012 by H. Eskandar et, al. [42]. This method is based on the natural principle of the water cycle and the flow of rivers and streams into the sea. The best population is considered as the sea and the solution during the search process is being updated with the stream to sea, stream to river, and river to the sea scheme as shown in Equation (9) - (11). The evaporation condition and raining process for a river to sea and stream to the sea are followed as per Equation (12) - (13) respectively, to update the raindrop array. The control parameters in three schemes were set following [42] and the detailed mathematical expression is explained as follows:

$$\mathbf{x}_{\mathrm{stream}} = \mathbf{x}_{\mathrm{stream}} + \mathrm{C}_1 \times \mathrm{rand} \times (\mathbf{x}_{\mathrm{sea}} - \mathbf{x}_{\mathrm{stream}}) \tag{9}$$

$$\mathbf{x}_{\mathrm{stream}} = \mathbf{x}_{\mathrm{stream}} + \mathrm{C}_2 \times \mathrm{rand} \times (\mathbf{x}_{\mathrm{river}} - \mathbf{x}_{\mathrm{stream}}) \tag{10}$$

$$\mathbf{x}_{\mathrm{river}} = \mathbf{x}_{\mathrm{river}} + \mathrm{C}_3 \times \mathrm{rand} \times (\mathbf{x}_{\mathrm{sea}} - \mathbf{x}_{\mathrm{river}}) \tag{11}$$

$$\mathbf{x}_{\mathrm{stream}} = \begin{cases} \mathbf{x}_{\mathrm{stream}} & ;\ \mathrm{norm}(\mathbf{x}_{\mathrm{river}} - \mathbf{x}_{\mathrm{sea}}) \geq \mathrm{D}_{\mathrm{max}} \text{ or rand } \geq \mathrm{C}_4 \\ \mathrm{rand}(\mathrm{nvar}, 1) & ;\ \mathrm{norm}(\mathbf{x}_{\mathrm{river}} - \mathbf{x}_{\mathrm{sea}}) < \mathrm{D}_{\mathrm{max}} \text{ or rand } < \mathrm{C}_4 \end{cases} \tag{12}$$

$$\mathbf{x}_{\mathrm{stream}} = \begin{cases} \mathbf{x}_{\mathrm{stream}} & ;\ \mathrm{norm}(\mathbf{x}_{\mathrm{stream}} - \mathbf{x}_{\mathrm{sea}}) \geq \mathrm{D}_{\mathrm{max}} \text{ or rand } \geq \mathrm{C}_4 \\ \mathrm{rand}(\mathrm{nvar}, 1) & ;\ \mathrm{norm}(\mathbf{x}_{\mathrm{stream}} - \mathbf{x}_{\mathrm{sea}}) < \mathrm{D}_{\mathrm{max}} \text{ or rand } < \mathrm{C}_4 \end{cases} \tag{13}$$

Where $\mathrm{C}_1 = 2$, is the constant parameter of "Moving stream to sea" scheme
$\mathrm{C}_2 = 2$, is the constant parameter of "Moving Streams to rivers" scheme
$\mathrm{C}_3 = 2$, is the constant parameter of "Moving rivers to Sea" scheme
$\mathrm{C}_4 = 0.1$, is the constant parameter of "Evaporation condition and raining process"
$\mathrm{D}_{\mathrm{max}}^{\mathrm{iter}+1} = \mathrm{D}_{\mathrm{max}}^{\mathrm{iter}} \times \frac{\mathrm{D}_{\mathrm{max}}^{\mathrm{iter}}}{\mathrm{iter}_{\mathrm{max}}}$; $\mathrm{D}_{\mathrm{max}}^{1} = 1\mathrm{e} - 16$

Finally, the next generation of the population can be selected from the current population and the updated population and assembled as per Equation (14)

$$\mathbf{x}_{WCA}^{iter+1} = \{\mathbf{x}_{sea}, \mathbf{x}_{river}, \mathbf{x}_{stream}\} \tag{14}$$

2.4 Population base increment learning

The last algorithm applied for the proposed hybrid algorithm in this work is Population base increment learning (PBIL). PBIL is a stochastic guided search method based on a probability matrix (P) with controlling parameters of the learning rate, search rate, and population size. Introduced by Beluja in 1994 [43], PBIL is a combination of generational GA mechanisms with a simple approach to competitive learning. The distribution of "1" and "0" digits in a binary population is represented and estimated by a probability vector. From this probability vector, new samples of candidate solutions can be extracted which eventually leads to next-generation solutions. PBIL algorithm starts with an initial probability vector $\mathrm{P} = \{0.5 , 0.5 , 0.5 , \ldots ,0.5 \}^T$ where the size of the probability matrix is equal to the total design variable (DSV) multiplied with binary length per DSV. For explanation, an example is illustrated in Table 1 which has 3 DSV with total 12-digit binary and total 6 solutions. The binary population (B) were generated randomly in the row direction based on the P and is used for computing the function evaluation and correspondingly update the new probability matrix (P^{iter+1}) in next generation following the Equation (15).

Table 1 Probability vectors and their corresponding populations

Probability vectors (P)		**Binary populations (B) (each column represents a binary design solution)**					
DSV no.1	0.5	1	0	1	0	1	0
	0.5	0	0	0	1	1	1
	0.5	1	1	1	0	0	0
	0.5	0	1	0	1	0	1
DSV no.2	0.5	0	0	0	1	1	1
	0.5	1	1	0	0	0	1
	0.5	0	1	1	0	0	1
	0.5	1	0	0	1	1	0
DSV no.3	0.5	1	0	0	1	1	0
	0.25	0	0	0	0	1	1
	0.0	0	0	0	0	0	0
	0.75	1	1	0	1	1	1

$$P^{iter+1} = P^{iter} \times (1 - L_R) + b \times L_R \tag{15}$$

Where, L_R represents the learning rate and b is the element representing the best binary solution. The learning rate function is assigned as:

$$L_R = 0.5 + rand \times (+0.1 \text{ or } -0.1) \tag{16}$$

2.5 Ensemble of the algorithms

The hybridized method proposed in this work viz. the ensemble of Genetic algorithm, Grey wolf optimiser, Water cycle algorithm, and Population base increment learning using weighted sum is based on the success weight archive methodology in which the population is divided into the subpopulations for each constituent algorithm. In the search process, the population initialization starts with a weight (W) of 0.25 for all optimizers, as shown in Equation (17).

$$W = \{0.25, 0.25, 0.25, 0.25\} \tag{17}$$

Four archive subpopulations are generated randomly and apply with the four algorithms stated above. The success archive and the success percentage were computed in selection procedures as shown in Figure 1, and then the new weight is updated by Equation (18).

$$W^{iter+1} = \frac{[\text{ArchS\_GA}, \ \text{ArchS\_GWO}, \ \text{ArchS\_WCA}, \ \text{ArchS\_PBIL}]}{\text{Success archive}} \tag{18}$$

Where ArchS_GA is the success archive of GA
ArchS_GWO is the success archive of GWO
ArchS_WCA is the success archive of WCA
ArchS_PBIL is the success archive of PBIL

3. Aeroelastic design problem

This work aims to explore an efficient metaheuristic for aircraft wing design problems. Figure 2 displays the composite structure of the Goland wing model. The model considered for the simulation process is separated into six individual components viz. spar, front spar, rear spar, 11 ribs, upper skin, and lower skin, as introduced by M. Goland [44]. In this work, the upper and lower skin were computed by using the composite material while the other parts were set as isotropic material (Details presented in Table 2). The details of the wing structure can be found in [45, 46]. In this study, the consideration of control surfaces and high lift devices is neglected. The considered wing model is subject to aerodynamic loadings, leading to the mutual interaction of three forces namely aerodynamic, elastic, and inertial forces. This structure/aerodynamic interaction of airframes is well known as aeroelasticity. It is prevalent in wing design that static and aerodynamic phenomena must be taken into account. For static aeroelasticity, a speed at which the aerodynamic loads overcome structural restoration or divergence speed must be avoided. The ratio of lift from cruise wing shape to that from its jig shape defined as lift effectiveness is considered as a design constraint. Flutter speed, a speed at which the aerodynamic stiffness and damping due to fluid/structure interaction resulting in wing dynamic instability, is also accounted as a restrain in the considered design model. In the proposed analysis, the wing encounter speed is considered following the flutter speed from Beran et al [46] (410 ft/s or ≈125 m/s) with 20 % avoidance (≈25 m/s). Thus the speed of the wind is set to be 100 m/s for analysis while the fuel and other storages were neglected for the wing.

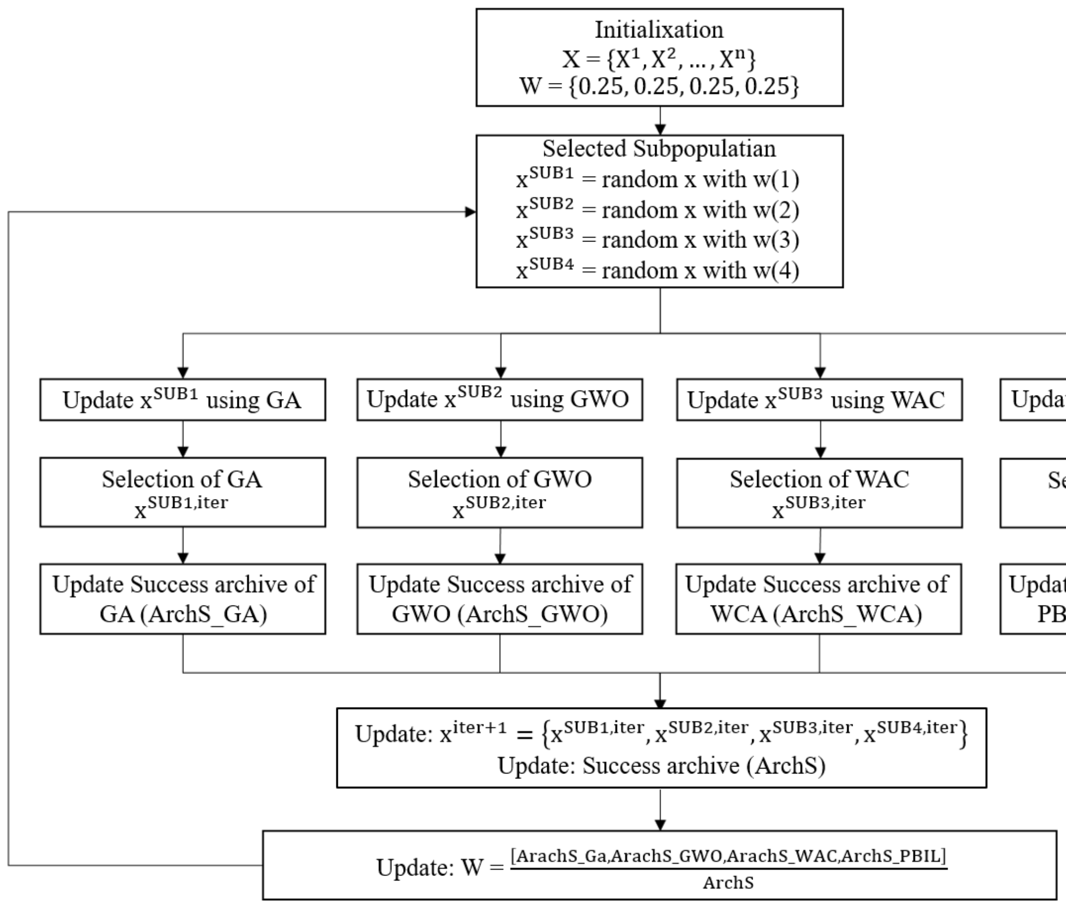

Figure 1 Ensemble of the four metaheuristics

Table 2 Mechanical properties used in the model

Material	Properties name	Value	Unit
Aluminium	Young's modulus (E)	70e+9	Pa.
	Poisson's ratio (ϑ)	0.3	-
	Density (ρ)	2700	kg/m^3
	Yield strength (S_y)	300e+6	Pa.
Carbon fibre	Young's modulus (E_{11})	207.7e+9	Pa.
	Young's modulus (E_{22})	7.6e+9	Pa.
	Shear modulus (G_{12})	5.0e+9	Pa.
	Shear modulus (G_{13})	5.0e+9	Pa.
	Shear modulus (G_{23})	5.0e+9	Pa.
	Major Poisson's ratio (ϑ)	0.3	-
	Density (ρ)	1800	kg/m^3
	Tensile strength (S_{ty11})	500e+6	Pa.
	Tensile strength (S_{ty22})	5e+6	Pa.
	Tensile strength (S_{ty12})	35e+6	Pa.
	Compression strength (S_{cy11})	350e+6	Pa.
	Compression strength (S_{cy22})	75e+6	Pa.
	Compression strength (S_{cy12})	35e+6	Pa.

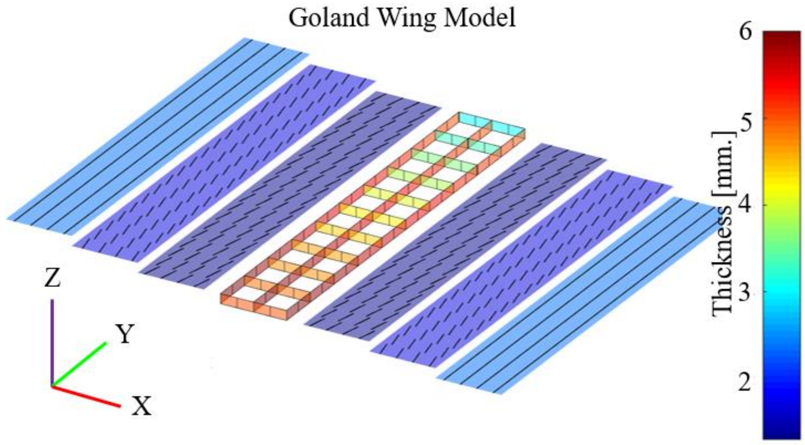

Figure 2 Composite plate geometry definition

The aero elastic optimization problem considered in this study can be mathematically modelled as:

$$\min_{\mathbf{x}} \mathrm{f}(\mathbf{x}) = \text{total wing mass} \tag{19}$$

Subject to
$$V_{al} - V_{cr} \leq 0 \tag{19.1}$$
$$\eta_L - \eta_{L,al} \leq 0 \tag{19.2}$$
$$u_{max} - u_{al} \leq 0 \tag{19.3}$$
$$t_{t,fs} - t_{r,fs} \leq 0 \tag{19.4}$$
$$t_{t,ms} - t_{r,ms} \leq 0 \tag{19.5}$$
$$t_{t,rs} - t_{r,rs} \leq 0 \tag{19.6}$$
$$t_{t,r} - t_{r,r} \leq 0 \tag{19.7}$$
$$\mathbf{x_l} \leq \mathbf{x} \leq \mathbf{x_u} \tag{19.8}$$

Where $\mathbf{x}$ represents a design variable vector having lower and upper bounds as $\mathbf{x}_L$ and $\mathbf{x}_U$ respectively; u_{max} and u_{al} presents the maximum and permissible transverse displacement on the wing; wing lift effectiveness is η_L that is the ratio of flexible to rigid total lift forces whereas $\eta_{L,al}$ represents its allowable value; V_{cr} and V_{al} are the critical (lowest of flutter and divergence speed) and allowable wind speed respectively; front spar thickness at the root and tip cord is $t_{r,fs}$ and $t_{t,fs}$ while for the middle spar, it is $t_{r,ms}$ and $t_{t,ms}$ respectively; similarly for the rear spar the thickness at the root and tip cord is presented as $t_{r,rs}$ and $t_{t,rs}$ while for the ribs, it is $t_{r,r}$ and $t_{t,r}$ respectively.

The objective function is set to minimize wing mass whereas the constraints are assigned so that the wing is safe from the static and dynamic aeroelastic phenomena. There is a total of 25 design variables accounted for in this investigation that can be separated into two sections. First is the thicknesses and ply orientations of composite skins (lower and upper) and the second one is the thickness and distribution function of isotropic material (structural part of Goland wing). The details of the design variables are as follows:

x_1 = distribution function of spar thickness
x_2 = thickness of spar at the root chord
x_3 = thickness of spar at tip chord
x_4 = distribution function of front spar thickness
x_5 = thickness of front spar at the root chord
x_6 = thickness of front spar at tip chord
x_7 = distribution function of rear spar thickness
x_8 = thickness of rear spar at the root chord
x_9 = thickness of rear spar at tip chord
x_{10} = distribution function of ribs location
x_{11} = distribution function of ribs thickess
x_{12} = thickness of ribs at the root chord
x_{13} = thickness of ribs at tip chord
x_{14-16} = thicknesses of laminated lower skin layers 1-3 (outside wing to inside wing)
x_{17-19} = orientations of laminated lower skin layers 1-3 (outside wing to inside wing)
x_{20-22} = thicknesses of laminated upper skin layers 1-3 (inside wing to outside wing)
x_{23-25} = orientations of laminated upper skin layers 1-3 (inside wing to outside wing)

In the above formulation, all design variables considered are of discrete nature. The thicknesses of composite layers are selected from {0.25, 0.5, 1.0, 1.3, 1.7, 2.4, 3.1, 3.4} mm while the ply orientations are limited to {-75, -60, -45, -30, -15, 0, 15, 30, 45, 60, 75, 90} degree. For the isotropic material, the thickness can be selected from {0.5, 0.7, 0.8, 1.0, 1.2, 1.5, 2, 2.5, 3, 4, 5, 6, 8, 10, 12, 15, 16, 20, 25, 30, 35, 40, 45, 50} mm. The three constraints above are set so that the wing moment of inertia with respect to the fuselage axis is lower to ease in lateral/directional motion control. The allowable constraint values are set as V_{al} = 200 m/s, u_{al} = 0.5 m, and $\eta_{L,al}$ = 0.9. following [46]. The quadrilateral Mindlin shell elements with drilling degree of freedom [47, 48] were used for modelling the finite element model while the shear correction factors are computed based on [49]. The vortex and doublet lattice method has been implemented for static and dynamic aerodynamic analysis. Moreover, quasi-unsteady aerodynamic forces are used for flutter analysis [50], which provides the results under an acceptable range in comparison to other available computational tools.

4. Experimental setup

To evaluate the performance of the E-GGWP-W algorithm, 18 constrained benchmark functions from the CEC-RW-2020 test suit are considered and contrasted with several established and newly developed MHs present in the literature. All benchmark functions are set at particular design conditions i.e. number of design variables, population size, and the total number of function evaluations (FEs) following Kumar, A et al. [37]. All the algorithms were executed for 30 independent runs for all problems. Moreover, all the considered algorithms are also explored to aeroelastic optimization of the composite Goland wing. Each optimizer is executed 10 times independently for this practical design example with the considered size of population 50 and 10,000 FEs. The design problem constraints are handled using the Kaveh-Zolghadr technique [51]. Friedman's test is used for statistically ranking all the MHs. The optimisers for comparative performance study considered in this study are Sine cosine algorithm (SCA) [52], Particle swarm optimisation (PSO) [53], Whale optimisation algorithm (WOA) [54], Dragonfly algorithm (DA) [55], Artificial bee colony (ABC) [56], Genetic algorithms (GA) [40], Grey wolf optimiser (GWO) [26] and Population base increment learning (PBIL) [43].

5. Results and discussion

For performance investigation based on the constrained mechanical CEC-RW-2020 benchmarks, the statistical results of the total 18 mechanical engineering problem functions (F15-30 and F32-33) are presented in Table A1 of the Appendix. The average, standard deviation, and Friedman's rank of optimum results are shown in which the standard deviation values are shown in the round brackets whereas Friedman's ranks are displayed in the square brackets. Outcomes demonstrate that the proposed algorithm E-GGWP-W is the best among all accounted algorithms according to Friedman's rank for 10 test functions. The second and third best algorithms are GWO and ABC that gives the best Friedman's rank results for 5 and 2 test problems, respectively. Friedman's ranks for mechanical constrained CEC2020 benchmark functions are averaged and reported in Table 3. It is found that E-GGWP-W has the best mean rank with 2.12037 while the second and third best optimizers are 2.75648 and 3.30833, respectively. The highest rank (worst) of 7.95741 was obtained by GA followed by PBIL and PSO with value 7.41019 and 7.05093 respectively.

Table 3 Summary of Friedman's test of constrained mechanical test problem in CEC-RW-2020 result with all SOEAs

Algorithm	Mean rank	Std rank	Total "rank 1"
SCA	5.63704	0.94171	0
PSO	7.05093	1.20742	0
WOA	4.58056	0.96637	0
DA	4.17870	1.24614	1
ABC	3.30833	1.34388	2
GA	7.95741	1.60596	0
GWO	2.75648	1.32123	5
PBIL	7.41019	0.68574	0
E-GGWP-W	2.12037	0.74322	10

The second investigation deals with the practical engineering problem. The competitive algorithms mentioned above have been applied in a variety of real engineering problems so far especially GA. GA is the most popular metaheuristic, which has been implemented on a number of design problems, for example, chemical engineering [57], heat transfer [58, 59], aerodynamic design [60, 61]. Moreover, other metaheuristics in the table have also been used in various engineering fields, for example, the energy engineering field [58, 59, 62-67] and computer science [68, 69]. This article is concerned with the aeroelastic optimization of the Golandwing, one of the most important aerospace engineering disciplines. The obtained optimum results by E-GGWP-W are presented in Table 4. Similarly using the proposed methodology, the optimal geometry obtained is illustrated in Figure 3 while the details of the optimum solution for aeroelastic phenomena which was found after the computational analysis is revealed in Table 5. The optimal overall wing weight obtained by the E-GGWP-W is 48.2125 kg with a critical speed of 236.2097 m/s. Moreover, while satisfying all design constraints the lift effectiveness and maximum transverse deflection value found by the proposed hybrid algorithm for the optimal wing is 1.0567 and 0.20379 m respectively.

The critical speed of the optimum solution is the divergence speed that is reasonable for lift effectiveness higher than 1.0. This phenomenon occurs when the wing has an extreme angle of attack subject to wing flexibility. The composite ply orientations at lower skin tend to be parallel with the span direction for supporting the high-pressure distribution from aerodynamic loadings. The outer layer has a higher thickness than the inner layers for the lower skin. For the position of ribs, they are aligned with more density at the root chord while with less density at the wing tip. This distribution solution is applying for supporting the high lift distribution similar to the skin thickness. The thickness of all three spars is thicker at the root chord and becomes thinner at the wing tip (DSV no. 2, 5, and 8 are more than no. 3, 6, and 9, respectively). The maximum thickness of the spar is at the front spar. For the upper skin, the orientations of three upper skin layers are, to some extent, antisymmetric to that of the lower skin. However, the thickness for each layer is different. The fiber orientations and thicknesses of the lower and upper wing skins are displayed in Figure 3.

Table 4 Optimum design results

DSV no.	Definition	value	unit
1	distribution function number	5	-
2	thickness of spar at root chord	2	mm.
3	thickness of spar at tip chord	0.8	mm.
4	distribution function number	1	-
5	thickness of front spar at root chord	15	mm.
6	thickness of front spar at tip chord	1.2	mm.
7	distribution function number	5	-
8	thickness of rear spar at root chord	3	mm.
9	thickness of rear spar at tip chord	1	mm.
10	distribution function number	1	-
11	distribution function number	1	-
12	thickness of ribs at root chord	1.2	mm.
13	thickness of ribs at root chord	0.5	mm.
14	thicknesses of laminated lower skin layers 1 (outer layer)	0.5	mm.
15	thicknesses of laminated lower skin layers 2 (middle layer)	0.25	mm.
16	thicknesses of laminated lower skin layers 3 (inner layer)	0.25	mm.
17	orientations of laminated lower skin layers 1 (outer layer)	-75	deg.
18	orientations of laminated lower skin layers 2 (middle layer)	75	deg.
19	orientations of laminated lower skin layers 3 (inner layer)	45	deg.
20	thicknesses of laminated upper skin layers 1 (inner layer)	0.25	mm.
21	thicknesses of laminated upper skin layers 2 (middle layer)	0.5	mm.
22	thicknesses of laminated upper skin layers 3 (outer layer)	0.25	mm.
23	orientations of laminated upper skin layers 1 (inner layer)	75	deg.
24	orientations of laminated upper skin layers 2 (middle layer)	15	deg.
25	orientations of laminated upper skin layers 3 (outer layer)	-75	deg.

Table 5 Optimum wing phenomenon

Parameter	value	unit
Total mass	48.2125	kg.
Divergence speed (V_d)	236.2097	m/s
Flutter speed (V_f)	307.1655	m/s
Critical speed (V_{cr})	236.2097	m/s
Lift effectiveness (η_L)	1.0567	-
Maximum deflection (u_{max})	0.20379	m.

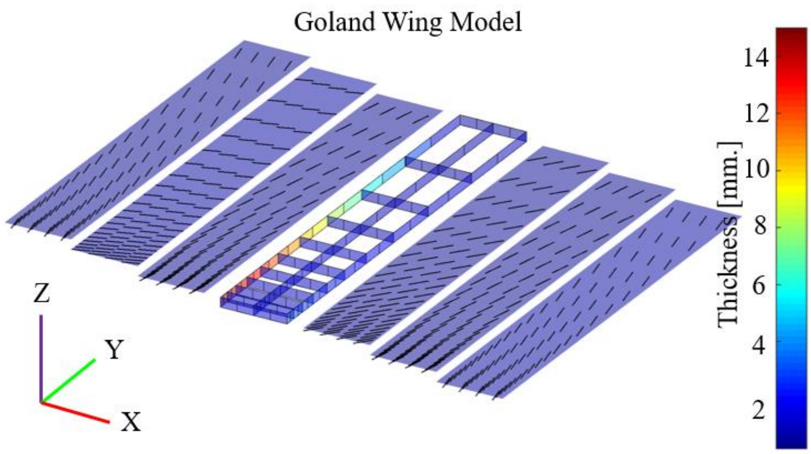

Figure 3 Optimum solution geometry model

6. Conclusions

The present study proposed and investigates a novel E-GGWP-W algorithm for the optimal design composite wing. In the proposed hybrid algorithm, GA, GWO, WCA, and PBIL MHs were used for the computation of subpopulations success archives, and accordingly, the weight is updated which eventually leads to solution modification. The suggested algorithm is explored for the benchmark functions of the CEC-RW-2020 test suit and composite Goland wing aeroelastic design to evaluate its performance. The simulation outcomes of the proposed algorithm are contrasted with eight distinguished algorithms subjected to the same input conditions. The results obtained reveal the dominance of E-GGWP-W over other considered algorithms. Moreover, based on Friedman's rank test carried out, E-GGWP-W ranked first for most of the design problems and shows its competency in solving real-life challenging optimization problems efficiently.

In the future, this algorithm can be explored for the higher dimension design optimization problem. Also, the interested scholar can extend this work for multi-modal and nonlinear practical challenging design problems with conflicting many objectives and evaluate the performance. Moreover, numerous comparison analysis can be performed with other existing prominent algorithms to achieve the best optimizer for a particular design problem.

7. Acknowledgements

The authors are grateful for the financial support provided by Defence Technology Institute (Public Organisation), The Royal Golden Jubilee Ph.D. Program (PHD/0182/2559), and The Thailand Research Found (RTA6180010).

8. References

[1] Wansaseub K, Sleesongsom S, Panagant N, Pholdee N, Bureerat S. Surrogate-assisted reliability optimization of an aircraft wing with static and dynamic aeroelastic constraints. Int J Aeronaut Sp Sci. 2020;21(3):723-32.
[2] Wansasueb K, Pholdee N, Panagant N, Bureerat S. Multiobjective meta-heuristic with iterative parameter distribution estimation for aeroelastic design of an aircraft wing. Eng Comput. 2020;1-19.
[3] Pathan MV, Patsias S, Tagarielli VL. A real-coded genetic algorithm for optimizing the damping response of composite laminates. Comput Struct. 2018;198:51-60.
[4] Nielsen MWD, Johnson KJ, Rhead AT, Butler R. Laminate design for optimised in-plane performance and ease of manufacture. Compos Struct. 2017;177:119-28.
[5] Zhao W, Gupta A, Regan CD, Miglani J, Kapania RK, Seiler PJ. Component data assisted finite element model updating of composite flying-wing aircraft using multi-level optimization. Aerosp Sci Technol. 2019;95:105486.
[6] Bureerat S. Apply optimization for mechanical engineering 1. Khon Kaen: KKU Printing House; 2013.
[7] Kumar S, Tejani GG, Mirjalili S. Modified symbiotic organisms search for structural optimization. Eng Comput. 2019;35: 1269-96.
[8] Tejani GG, Kumar S, Gandomi AH. Multi-objective heat transfer search algorithm for truss optimization. Eng Comput. 2019;1: 1-22.
[9] Yildiz AR, Abderazek H, Mirjalili S. Correction to: a comparative study of recent non-traditional methods for mechanical design optimization. Arch Comput Meth Eng. 2019;1:3.
[10] Yildiz BS. A comparative investigation of eight recent population-based optimization algorithms for mechanical and structural design problems. Int J Veh Des. 2017;73:208-18.
[11] Abderazek H, Yildiz AR, Mirjalili S. Comparison of recent optimization algorithms for design optimization of a cam-follower mechanism. Knowledge-Based Syst. 2020;191:105237.
[12] Yildiz BS, Yildiz AR. Comparison of grey Wolf, whale, water cycle, ant lion and sine-cosine algorithms for the optimization of a vehicle engine connecting rod. Mater Test. 2018;60:311-5.
[13] Yıldız BS. Optimal design of automobile structures using moth-flame optimization algorithm and response surface methodology. Mater Test. 2020;62:371-7.
[14] Yıldız BS. The spotted hyena optimization algorithm for weight-reduction of automobile brake components. Mater Test. 2020;62:383-8.
[15] Yıldız BS, Yıldız AR, Albak EI, Abderazek H, Sait S, Bureerat S. Butterfly optimization algorithm for optimum shape design of automobile suspension components. Mater Test. 2020;62(4):365-70.
[16] Hamza F, Abderazek H, Lakhdar S, Ferhat D, Yıldız AR. Optimum design of cam-roller follower mechanism using a new evolutionary algorithm. Int J Adv Manuf Tech. 2018;99:1267-82.
[17] Yildiz BS. Natural frequency optimization of vehicle components using the interior search algorithm. Mater Test. 2017;59: 456-8.
[18] Meng Z, Li G, Wang X, Sait SM, Yıldız AR. A comparative study of metaheuristic algorithms for reliability-based design optimization problems. Arch Comput Methods Eng. 2020;28(4):1853-69.
[19] Yıldız AR, Yıldız BS, Sait SM, Li X. The Harris hawks, grasshopper and multi-verse optimization algorithms for the selection of optimal machining parameters in manufacturing operations. Mater Test. 2019;8(61):1-15.
[20] Yildiz AR. A novel hybrid whale-Nelder-Mead algorithm for optimization of design and manufacturing problems. Int J Adv Manuf Tech. 2019;105:5091-104.
[21] Zhang L, Ma D, Yang M, Wang S. Optimization and analysis of winglet configuration for solar aircraft. Chinese J Aeronaut. 2020;33(12):3238-52.
[22] Shrivastava S, Mohite PM, Yadav T, Malagaudanavar A. Multi-objective multi-laminate design and optimization of a Carbon Fibre Composite wing torsion box using evolutionary algorithm. Compos Struct. 2018;185:132-47.
[23] Tao J, Sun G, Guo L, Wang X. Application of a PCA-DBN-based surrogate model to robust aerodynamic design optimization. Chinese J Aeronaut. 2020;33(6):1573-88.
[24] Jafari S, Nikolaidis T. Meta-heuristic global optimization algorithms for aircraft engines modelling and controller design; a review, research challenges, and exploring the future. Progr Aero Sci. 2019;104:40-53.
[25] Wolpert DH, Macready WG. No free lunch theorems for optimization. IEEE Trans Evol Comput. 1997;1:67-82.
[26] Mirjalili S, Mirjalili SM, Lewis A. Grey wolf optimizer. Adv Eng Softw. 2014;69:46-61.
[27] Hertz A, de Werra D. Using tabu search techniques for graph coloring. Comput. 1987;39:345-51.
[28] Kuik R, Salomon M, Van Wassenhove LN, Maes J. Linear programming, simulated annealing and tabu search heuristics for lotsizing in bottleneck assembly systems. IIE Trans Institute Ind Eng. 1993;25:62-72.
[29] Lee JK, Kim YD. Search heuristics for resource constrained project scheduling. J Oper Res Soc. 1996;47:678-89.
[30] Yang X-S. Review of metaheuristics and generalized evolutionary walk algorithm. Int J Bio-Inspired Comput. 2011;3:77-84.
[31] Rashedi E, Nezamabadi-pour H, Saryazdi S. GSA: a gravitational search algorithm. Inf Sci (Ny) 2009;179:2232-48.

[32] Sorensen K. Metaheuristics-the metaphor exposed. Int Trans Oper Res. 2015;22:3-18.
[33] Mernik M, Liu S-H, Karaboga D, Crepinsek M. On clarifying misconceptions when comparing variants of the Artificial Bee Colony Algorithm by offering a new implementation. Inf Sci. 2015;291:115-27.
[34] Crepinsek M, Liu SH, Mernik M. Replication and comparison of computational experiments in applied evolutionary computing: Common pitfalls and guidelines to avoid them. Appl Soft Comput J. 2014;19:161-70.
[35] Kumar S, Tejani GG, Pholdee N, Bureerat S. Multi-objective modified heat transfer search for truss optimization. Eng Comput. 2020:1-16.
[36] Kumar S, Tejani GG, Pholdee N, Bureerat S. Improved metaheuristics through migration-based search and an acceptance probability for truss optimization. Asian J Civ Eng. 2020;21:1217-37.
[37] Kumar A, Wu G, Ali MZ, Mallipeddi R, Suganthan PN, DAS S. A test-suite of non-convex constrained optimization problems from the real-world and some baseline results. Swarm Evol Comput. 2020;56:100693.
[38] Holland JH. Adaptation in natural and artificial systems. University of Michigan: The MIT Press; 1975.
[39] Sampson JR. Adaptation in natural and artificial systems (John H. Holland). SIAM Rev. 1976;18:529-30.
[40] Sastry K, Goldberg D, Kendall G. Genetic algorithms. In: Burke EK, Kendall G, editors. Search methodologies. USA: Springer; 2014. p. 97-125.
[41] Grefenstette JJ. Optimization of control parameters for genetic algorithms. IEEE Trans Syst Man Cybern. 1986;16:122-8.
[42] Eskandar H, Sadollah A, Bahreininejad A, Hamdi M. Water cycle algorithm-a novel metaheuristic optimization method for solving constrained engineering optimization problems. Comput Struct. 2012;110-111:151-66.
[43] Hughes EJ. Optimisation using population based incremental learning (PBIL). IEE Colloquium on Optimisation in Control: Methods and Applications; 1998 Nov 10; London, UK. London: IET; 2002.
[44] Goland M. The flutter of a uniform cantilever wing. J Appl Mech. 1945;12:A197-208.
[45] Beran PS, Strganac TW, Kim K, Nichkawde C. Studies of store-induced limit-cycle oscillations using a model with full system nonlinearities. Nonlinear Dyn. 2004;37(4):323-39.
[46] Beran PS, Khot NS, Eastep FE, Snyder RD, Zweber JV. Numerical analysis of store-induced limit-cycle oscillation. J Aircr. 2004;41(6):1315-26.
[47] Kefal A, Tessler A, Oterkus E. An enhanced inverse finite element method for displacement and stress monitoring of multilayered composite and sandwich structures. Compos Struct. 2017;179:514-40.
[48] Nguyen-Van H, Mai-Duy N, Karunasena W, Tran-Cong T. Buckling and vibration analysis of laminated composite plate/shell structures via a smoothed quadrilateral flat shell element with in-plane rotations. Comput Struct. 2011;89(7-8):612-25.
[49] Figueiras JA. Ultimate load analysis of anisotropic and reinforced concrete plates and shells [dissertation]. Wales: Swansea University; 1983.
[50] Katz J, Plotkin A. Low-speed aerodynamics. 2nd ed. USA: Cambridge University Press; 2004.
[51] Kaveh A, Zolghadr A. Truss optimization with natural frequency constraints using a hybridized CSS-BBBC algorithm with trap recognition capability. Comput Struct. 2012;102-103:14-27.
[52] Mirjalili S. SCA: A sine cosine algorithm for solving optimization problems. Knowledge-Based Syst. 2016;96:120-33.
[53] Wang D, Tan D, Liu L. Particle swarm optimization algorithm: an overview. Soft Comput. 2018;22:387-408.
[54] Mirjalili S, Lewis A. The whale optimization algorithm. Adv Eng Softw. 2016;95:51-67.
[55] Mirjalili S. Dragonfly algorithm: a new meta-heuristic optimization technique for solving single-objective, discrete, and multi-objective problems. Neural Comput Appl. 2016;27:1053-73.
[56] Karaboga D, Basturk B. On the performance of artificial bee colony (ABC) algorithm. Appl Soft Comput J. 2008;8:687-97.
[57] Kim C, Batra R, Chen L, Tran H, Ramprasad R. Polymer design using genetic algorithm and machine learning. Comput Mater Sci. 2021;186:110067.
[58] Liu C, Bu W, Xu D. Multi-objective shape optimization of a plate-fin heat exchanger using CFD and multi-objective genetic algorithm. Int J Heat Mass Transf. 2017;111:65-82.
[59] Prieler R, Mayrhofer M, Gaber C, Gerhardtera H, Schlucknera C, Landfahrera M, et al. CFD-based optimization of a transient heating process in a natural gas fired furnace using neural networks and genetic algorithms. Appl Therm Eng. 2018;138:217-34.
[60] Gao Y, Tian Y, Liu H, Sun X. Gaussian fitting based optimal design of aircraft mission success space using multi-objective genetic algorithm. Chinese J Aeronaut. 2020;33(12):3318-30.
[61] Hu Y, Yang Y, Li S, Zhou Y. Fuzzy controller design of micro-unmanned helicopter relying on improved genetic optimization algorithm. Aerosp Sci Tech. 2020;98(9):105685.
[62] Samadianfard S, Hashemi S, Kargar K, Izadyar M, Mostafaeipour A, Mosavi A, et al. Wind speed prediction using a hybrid model of the multi-layer perceptron and whale optimization algorithm. Energ Rep. 2020;6:1147-59.
[63] Chen H, Li W, Yang X. A whale optimization algorithm with chaos mechanism based on quasi-opposition for global optimization problems. Expert Syst Appl. 2020;158:113612.
[64] Naserbegi A, Aghaie M, Zolfaghari A. Implementation of grey wolf optimization (GWO) algorithm to multi-objective loading pattern optimization of a PWR reactor. Ann Nucl Energy. 2020;148:107703.
[65] Singh S, Chauhan P, Singh NJ. Capacity optimization of grid connected solar/fuel cell energy system using hybrid ABC-PSO algorithm. Int J Hydrogen Energy. 2020;45:10070-88.
[66] Silva MH Da, Schirru R. Optimization of nuclear reactor core fuel reload using the new quantum PBIL. Ann Nucl Energy. 2011;38:610-4.
[67] da Silva MH, Legey AP, de Mol AC. The evolution of PBIL algorithm when used to solve the nuclear reload optimization problem. Annals Nucl Energy. 2018;113:393-8.
[68] Yu C, Cai Z, Ye X, Wang M, Zhao X, Liang G, et al. Quantum-like mutation-induced dragonfly-inspired optimization approach. Math Comput Simul. 2020;178:259-89.
[69] Shilaja C, Arunprasath T. Internet of medical things-load optimization of power flow based on hybrid enhanced grey wolf optimization and dragonfly algorithm. Futur Gener Comput Syst. 2019;98:319-30.

Appendix

A comparative performance of MHs on the constrained CEC-RW-2020 functions

Table A1 Comparative of constrained CEC-RW-2020 results of all MHs

Mean (Std) [Friedman's rank]	SCA	PSO	WOA	DA	ABC
CECRW2020	3010.55300	3874.20440	3012.91146	3016.54598	2994.23425
F15	(5.06589)	(800.17722)	(15.83280)	(19.41488)	(0.00000)
Weight Minimization of a Speed Reducer	[5.06667]	[7.60000]	[4.90000]	[5.13333]	[1.60000]
CECRW2020	6.25376	3.76376e+06	14068.33019	3749.47683	0.06364
F16	(1.88244)	(2.92487e+06)	(36528.28553)	(17984.88723)	(0.01177)
Optimal Design of Industrial refrigeration System	[6.20000]	[9]	[4.56667]	[6.26667]	[2.70000]
CECRW2020	0.01502	6.59165	0.01370	0.01490	0.01284
F17	(0.00263)	(35.82178)	(0.00125)	(0.00535)	(0.00013)
Tension/compression spring design (case 1)	[4.80000]	[8.10000]	[4.73333]	[4.66667]	[3.53333]
CECRW2020	6961.98232	8164.33398	6602.35688	6460.06826	5774.37631
F18	(1738.66474)	(2798.83763)	(487.40702)	(529.71925)	(35.60709)
Pressure vessel design	[5.40000]	[6.10000]	[5.43333]	[4.83333]	[2.63333]
CECRW2020	1.85639	2.41816	1.86778	1.78673	1.88771
F19	(0.01461)	(0.47156)	(0.22552)	(0.14669)	(0.08876)
Welded beam design	[4.86667]	[7.03333]	[4.60000]	[3.53333]	[5.50000]
CECRW2020	263.86200	264.17989	263.96738	263.85279	263.87665
F20	(0.00905)	(1.20750)	(0.16526)	(0.00092)	(0.02697)
Three-bar truss design problem	[5.20000]	[3.30000]	[6.16667]	[3.36667]	[5.70000]
CECRW2020	0.23525	0.28170	0.23525	0.23720	0.23524
F21	(0.00000)	(0.06297)	(0.00001)	(0.00746)	(0.00000)
Multiple disk clutch brake design problem	[4.90000]	[7.61667]	[3.60000]	[2.06667]	[4.16667]
CECRW2020	1.50001e+05	7.30262e+05	0.59090	0.56925	0.53347
F22	(3.41144e+05)	(3.32063e+06)	(0.12788)	(0.09237)	(0.00474)
Planetary gear train design optimization problem	[7.21667]	[7.73333]	[3.73333]	[4.10000]	[2.56667]
CECRW2020	26.56827	710.14610	17.97876	23.96788	16.05397
F23	(3.77828)	(949.94962)	(5.02367)	(5.17601)	(0.01164)
Step-cone pulley problem	[5.76667]	[6.73333]	[3.93333]	[5.20000]	[2.13333]
CECRW2020	6.73097	26123.61530	5.51372	5.11324	4.09662
F24	(2.14981)	(1.05261e+05)	(1.42285)	(1.29878)	(0.52820)
Robot gripper problem	[6.05000]	[7.40000]	[4.80000]	[4.48333]	[3]
CECRW2020	3.94203e+05	2755.07901	306.14570	603.31101	665.28706
F25	(1.16933e+06)	(693.14390)	(166.69668)	(319.42885)	(252.39881)
Hydro-static thrust bearing design problem	[5.76667]	[6.83333]	[2.26667]	[4.10000]	[4.46667]
CECRW2020	4.54960e+08	2.03760e+09	5.84887e+07	1.87798e+08	1.11571e+06
F26	(1.08197e+09)	(4.57847e+09)	(4.24723e+07)	(1.30446e+08)	(1.13988e+06)
Four-stage gear box problem	[6.03333]	[7.70000]	[4.26667]	[5.66667]	[1.36667]
CECRW2020	576.03223	588.38240	561.09711	535.11936	523.11842
F27	(39.50365)	(25.82150)	(20.43125)	(9.81908)	(0.41605)
10-bar truss design	[6.20000]	[7.20000]	[5.93333]	[3.90000]	[1.96667]
CECRW2020	17771.59491	45120.92238	18258.95847	17352.83597	16949.69172
F28	(1571.27721)	(76391.57487)	(3510.60211)	(555.57731)	(0.00178)
Rolling element bearing	[5.63333]	[7.33333]	[4.76667]	[4.33333]	[1.90000]
CECRW2020	3.16674e+06	3.50551e+06	3.05154e+06	3.11528e+06	3.01208e+06
F29	(29840.92018)	(1.46551e+06)	(99470.38821)	(91229.55972)	(42168.67052)
Gas Transmission Compressor Design (GTCD)	[6.76667]	[5.46667]	[4.10000]	[5.30000]	[3.80000]
CECRW2020	2.72860	3.54802	2.96317	2.88845	2.76662
F30	(0.08015)	(0.72860)	(0.24592)	(0.35073)	(0.08517)
Tension/compression spring design (case 2)	[3.63333]	[6.76667]	[5.56667]	[3.86667]	[4.23333]
CECRW2020	-3.04427e+04	-2.98785e+04	-3.03483e+04	-3.05871e+04	-3.04242e+04
F32	(346.11979)	(360.41721)	(311.01908)	(118.24991)	(85.37811)
Himmelblau's Function	[4.63333]	[7.36667]	[5.50000]	[3.26667]	[5.20000]
CECRW2020	3.54955	3.81490	2.63935	2.63935	2.63935
F33	(0.38616)	(0.47338)	(0)	(0.00000)	(0.00000)
Topology Optimization	[7.33333]	[7.63333]	[3.58333]	[1.13333]	[3.08333]

* The best Friedsman' rank is present in bold

Table A1 (continued) Comparative of constrained CEC-RW-2020 results of all MHs

Mean (Std) [Friedman's rank]	GA	GWO	PBIL	E-GGWP-W
CECRW2020	9.55489e+09	2997.63320	4772.26087	2994.23425
F15	(9.90305e+09)	(2.03848)	(3582.65018)	(0.00000)
Weight Minimization of a Speed Reducer	[8.93333]	[3.03333]	[7.33333]	[1.40000]
CECRW2020	2089.89356	0.03850	47663.72085	3121.03272
F16	(10097.53243)	(0.00222)	(1.16687e+05)	(17092.82767)
Optimal Design of Industrial refrigeration System	[5.26667]	[1.20000]	[7]	[2.80000]
CECRW2020	13017.73275	0.01268	0.02128	0.01283
F17	(28038.70719)	(0.00001)	(0.00666)	(0.00020)
Tension/compression spring design (case 1)	[7.50000]	[1.20000]	[7.26667]	[3.20000]
CECRW2020	9.90992e+16	5878.97125	8732.18319	6050.64263
F18	(6.46346e+16)	(417.04159)	(2595.27319)	(428.80456)
Pressure vessel design	[8.46667]	[2]	[7.30000]	[2.83333]
CECRW2020	3.67325e+19	1.68533	2.54168	1.67171
F19	(1.72764e+20)	(0.04374)	(0.57644)	(0.00294)
Welded beam design	[8.86667]	[1.86667]	[7.50000]	[1.23333]
CECRW2020	Inf	263.85236	265.35004	263.85235
F20	(NaN)	(0.00002)	(2.20340)	(0.00000)
Three-bar truss design problem	[9]	[2.93333]	[7.83333]	[1.50000]
CECRW2020	2.73541e+05	0.23526	0.23836	0.23524
F21	(1.49825e+06)	(0.00001)	(0.00311)	(0.00000)
Multiple disk clutch brake design problem	[7.81667]	[5.70000]	[7.51667]	[1.61667]
CECRW2020	6667203152216713	0.53415	3334.30627	0.53555
F22	(2.53707e+16)	(0.00449)	(18257.38309)	(0.00789)
Planetary gear train design optimization problem	[6.73333]	[2.76667]	[7.33333]	[2.81667]
CECRW2020	1.18834e+11	16.04733	1.78323e+09	16.52140
F23	(7.33504e+09)	(0.00164)	(2.52693e+09)	(0.46265)
Step-cone pulley problem	[9]	[1.73333]	[8]	[2.50000]
CECRW2020	8.56971e+12	4.02070	1.24380e+07	3.64509
F24	(4.69380e+13)	(0.99018)	(6.81258e+07)	(0.81299)
Robot gripper problem	[5.70000]	[3.05000]	[8.50000]	[2.01667]
CECRW2020	5.98174e+24	364.31167	2.35963e+05	258.95817
F25	(3.12281e+25)	(107.68192)	(5.02887e+05)	(187.35940)
Hydro-static thrust bearing design problem	[9]	[2.76667]	[7.76667]	[2.03333]
CECRW2020	4.88417e+16	1.59058e+07	1.82214e+08	9.54464e+06
F26	(8.76552e+16)	(1.24924e+07)	(1.36679e+08)	(1.31668e+07)
Four-stage gear box problem	[9]	[2.86667]	[6]	[2.10000]
CECRW2020	1.07745e+05	523.94307	575.73592	525.84862
F27	(1.18192e+05)	(1.94992)	(21.80035)	(3.07346)
10-bar truss design	[8.86667]	[1.93333]	[6.63333]	[2.36667]
CECRW2020	1.50237e+07	17001.93367	22127.39323	16957.09107
F28	(8.19284e+06)	(45.02959)	(3200.29261)	(25.67121)
Rolling element bearing	[8.70000]	[3.76667]	[7.40000]	[1.16667]
CECRW2020	6.39614e+12	2.96661e+06	3.33967e+06	2.98909e+06
F29	(7.61987e+12)	(7076.36475)	(2.32161e+05)	(63113.63107)
Gas Transmission Compressor Design (GTCD)	[8.80000]	[1.76667]	[7.30000]	[1.70000]
CECRW2020	9.68896e+23	2.69622	896.77876	2.70526
F30	(1.28584e+24)	(0.08602)	(4882.06594)	(0.08648)
Tension/compression spring design (case 2)	[9]	[2.53333]	[7.13333]	[2.26667]
CECRW2020	3.95408e+10	-3.06623e+04	-3.01005e+04	-3.06655e+04
F32	(2.00346e+10)	(2.16853)	(267.02734)	(0.00000)
Himmelblau's Function	[9]	[2.46667]	[6.56667]	[1]
CECRW2020	2.63935	2.79931	7.07484	2.64105
F33	(0)	(0.10001)	(0.81432)	(0.00547)
Topology Optimization	[3.58333]	[6.03333]	[9]	[3.61667]

* The best Friedsman’ rank is present in bold